Figure S1

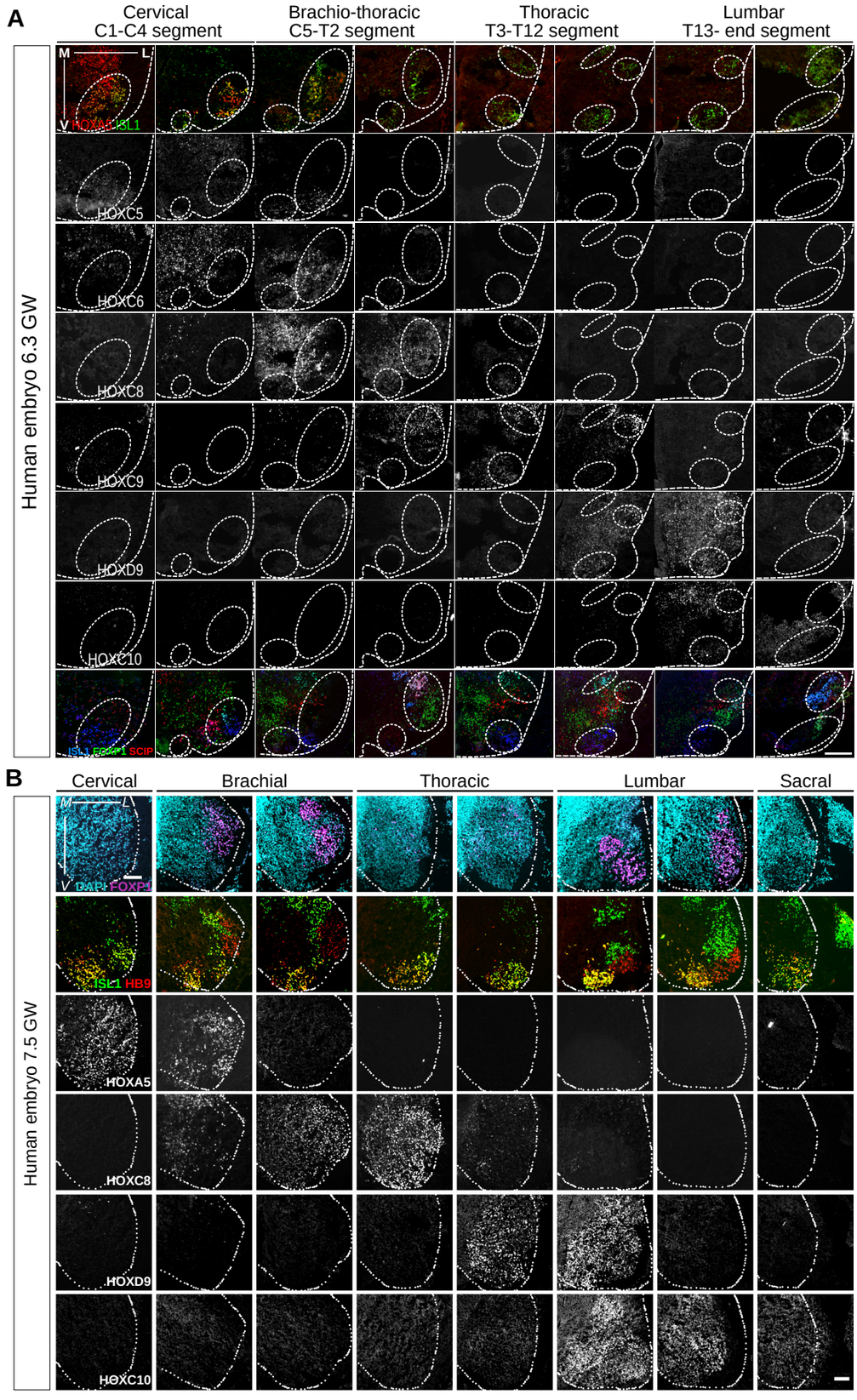

Figure S1 - Rostro-caudal distribution of motor neuron subtypes in human embryonic spinal cords. Related to Figure 1A

Immunostaining on transverse sections of human embryonic spinal cords at gestation weeks (GW) 6.3 **(A)** and 7.5 **(B)** to define HOX and MN subtype markers expression profiles in spinal MNs. MNs organized in motor columns that innervate distinct muscle groups were identified by their localization in the ventral horn and the expression of ISL1 or HB9. HOXA/C5 MNs are localized in the cervical regions, while HOXC6, HOXC9 and HOXC10 MNs are respectively at brachial, thoracic and lumbar levels. HOXC8 MNs are in the caudal brachial region and the anterior thoracic domain where some MNs co-express HOXC9. HOXD9 MNs are in the caudal thoracic and the anterior lumbar regions. FOXP1high MNs form lateral motor columns at brachial, anterior thoracic and lumbar levels which correspond to limb innervating MNs in mouse (Dasen et al., 2008; , Rousso et al., 2008). FOXP1high/SCIPhigh MNs are present in the caudal brachial and anterior thoracic regions which respectively characterize forearm and forepaw innervating MNs in mouse (Dasen et al., 2008, Mendelsohn et al., 2017). External dotted lines in A and B mark the side of the ventral horn. M: medial L: lateral V: Ventral. Scale bars : 100µm.

Figure S2

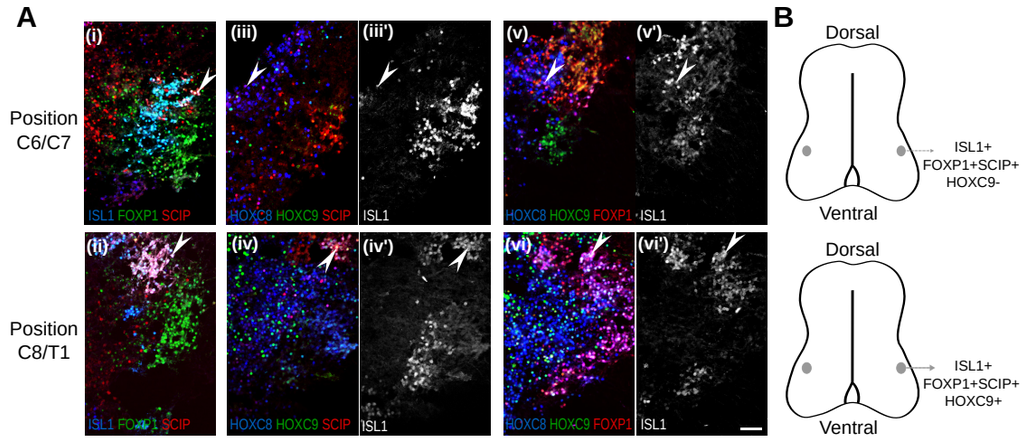

Figure S2 – Characterization of brachial and anterior thoracic FOXP1/SCIP MN subtypes
(A) Arrows in i) and ii) indicate FOXP1/SCIP/ISL1 MNs in caudal brachial and anterior thoracic spinal cord. Arrows in iii) and v) point to the presence of HOXC9-negative FOXP1/HOXC8/ISL1-positive MNs (ISL1 shown in iii' and v'). In iv, iv' and vi, vi', SCIP/ISL1 or FOXP1/ISL1 MNs around and caudal to the caudal brachial/anterior thoracic border co-expressed HOXC8 and HOXC9, which correspond to digit innervating MNs in mouse (Mendelsohn et al., 2017). **(B)** Schematic representation of the FOXP1/SCIP/ISL1/HOXC8 and FOXP1/SCIP/ISL1/HOXC9 MNs in brachial and thoracic regions. Scale bar: 100µm.

Figure S3

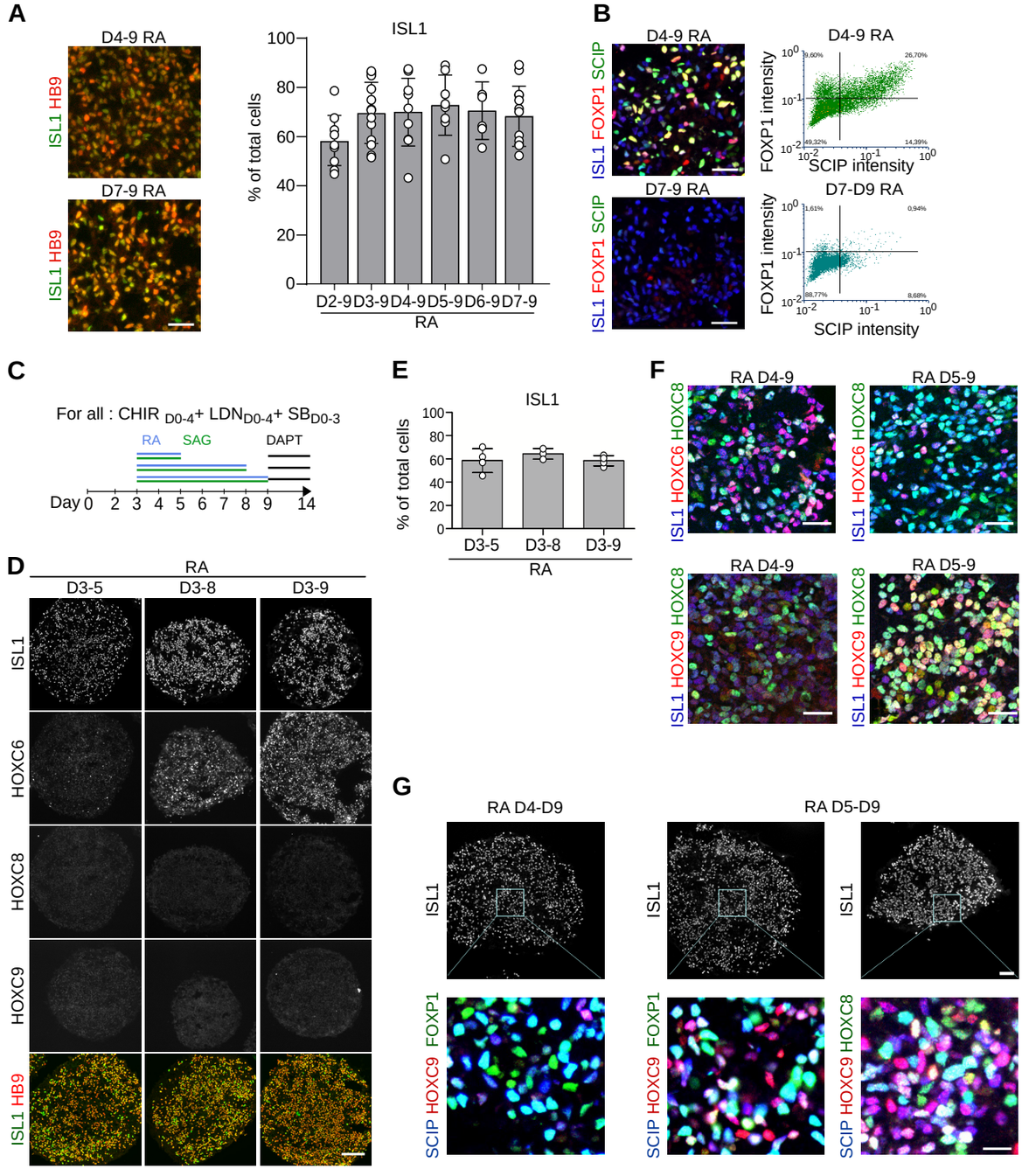

Figure S3 - The timing of exposure to RA and not the exposure duration controls the specification of caudal motor neurons from hESC and hiPSC. *Related to Figure 1*

(A) Proportion of MNs generated on Day 14 of differentiation when modulating the Day at which RA/SAG is added. Scale bar: 30µm. **(B)** Quantification of FOXP1high and FOXP1high/SCIP MNs. Intensity of FOXP1 and SCIP staining in all ISL1+ cells were extracted using Cell Profiler software. Intensity plots were generated for all conditions. FOXP1 and SCIP weak or negative cells were defined on the D7-D9 RA condition. Scale bar: 30µm. **(C-E)** Characterization on Day 14 of differentiation of the effect of varying RA/SAG duration of exposure on MN subtypes identity. **(C)** Differentiation conditions. **(D)** Immunostaining on cryostat sections of EBs for ISL1 and HOXs showing the absence of caudal HOXs when RA is added on Day 3 and the duration of exposure modulated. Scale bar: 100 µm. **(E)** Proportion of MNs (ISL1+ cells, mean ± SD) generated on Day 14 in the three tested conditions. **(F)** Immunostaining on cryostat sections of Day 14 EBs for the indicated markers quantified in Fig. 1D-F. Scale bar : 30µm. **(G)** Immunostaining on cryostat sections of EBs showing the presence of HOXC8/HOXC9/SCIP/ISL1 MNs and HOXC9/SCIP/FOXP1/ISL1 MNs that correspond to forepaw innervating-MNs in mouse and might represent hand innervating MNs in human. Scale bar: 40µm (top) and 15µm (bottom). Data are shown as mean ± SD. Each circle is an independent biological replicate: n=6 to 13 (A), n=3 to 4 (E). * if $P \leq 0.05$, ** if $P \leq 0.01$ and *** if $P \leq 0.001$. ANOVA with KW post hoc.

Figure S4

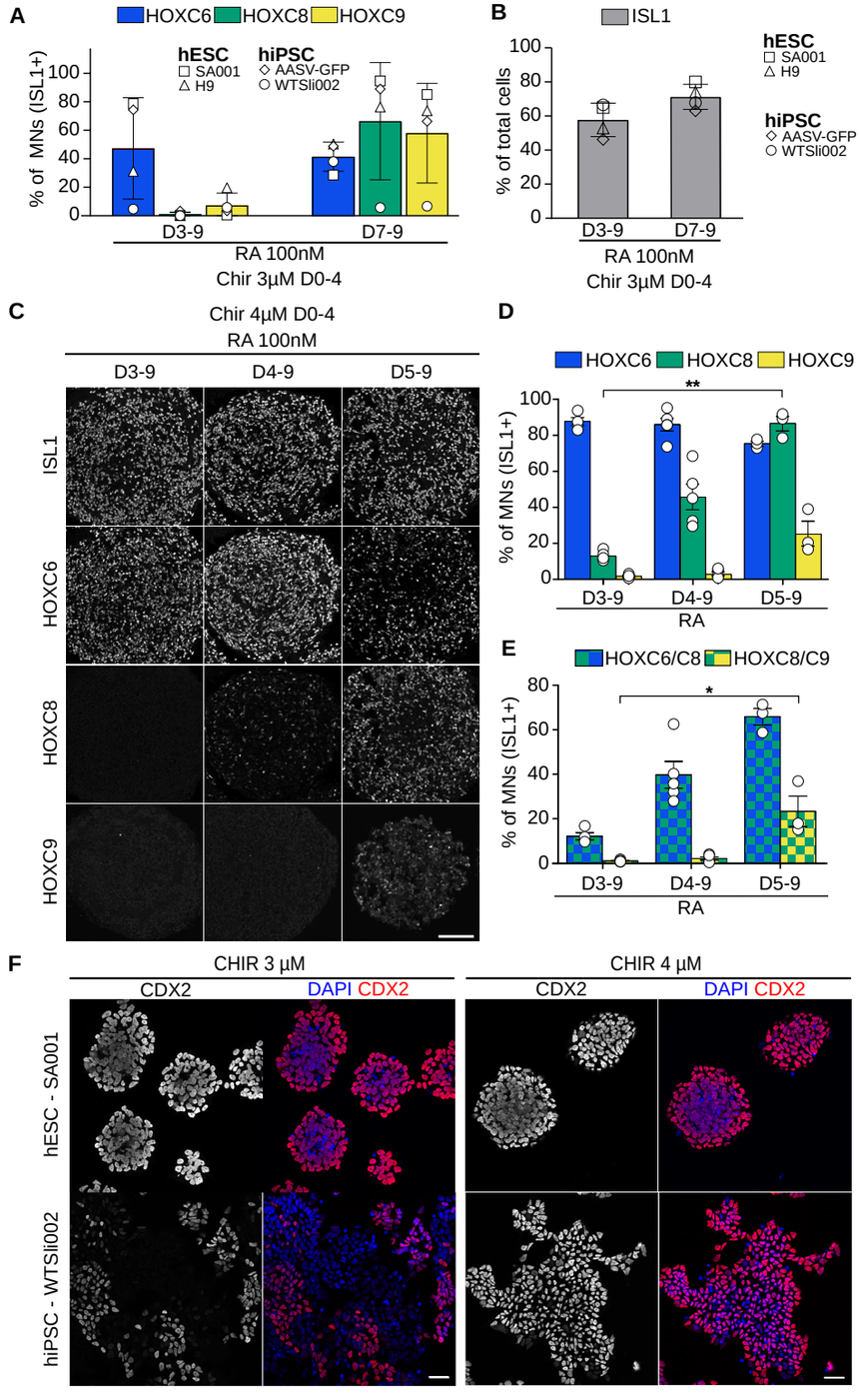

Figure S4 - The concentration of exposure to WNT agonist impacts the axial specification of stem cells and varies according cell lines. *Related to Figure1*

(A) Quantification of HOXC6-9 immunostaining on Day 14 cryostat sections of EBs derived from different hESC (SA001 and H9) and hiPSC (AASV-GFP and WTSli002). Cells were exposed to CHIR99021 (CHIR) 3µM together with LDN193189 from Day 0 to 4, and SB431542 from Day 0 to 3, then RA 100nM was alternatively applied from Day 3 or Day 7, up to Day 9. EBs derived from WTSli002 line do not express caudal HOXs when treated with the usual concentration of CHIR 3µM. **(B)** Quantification of ISL1+ cells on immunostaining on Day 14 cryostat sections of Day 14 EBs derived from different hPSC lines as presented in (A). **(C)** Immunostaining on cryostat sections of D14 hiPSC (WTSli002)-derived EBs for HOXs showing the generation of HOXC8 and then HOXC9 MNs when addition of RA is delayed. Cells were exposed to CHIR 4µM together with LDN193189 from Day 0 to 4, and SB431542 from Day 0 to 3, then RA 100nM was alternatively applied from Day 3, 4 or 5, up to Day 9. Scale bar: 100 µm. **(D-E)** Quantification of indicated markers on immunostaining on Day 14 EBs cryostat sections. **(F)** Immunostaining on Day 3 EBs plated on matrigel coated coverslips, derived from hESC line SA001 or hiPSC line WTSli002. EBs were exposed either to CHIR 3 or 4 µM on Day 0 of differentiation together with LDN193189 and SB431542. Scale bar: 40 µm. Data are shown as mean ± SD. Each circle is an independent biological replicate: n=3 to 5 (D-E). * if $P \leq 0.05$ and ** if $P \leq 0.01$. ANOVA with KW post hoc.

Figure S5

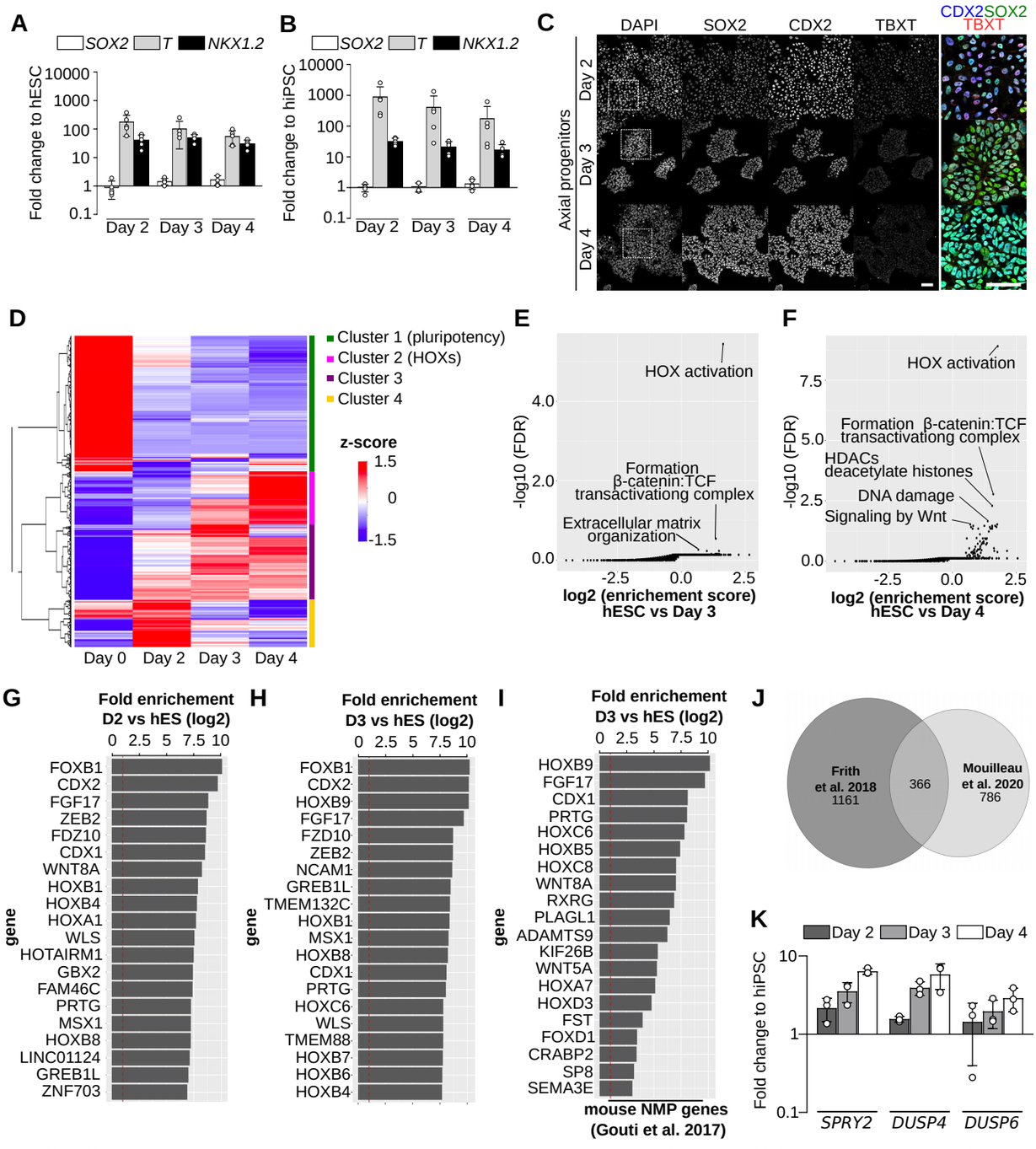

Figure S5 -Similarity between axial progenitors derived from hESC and hiPSC and mouse NMPs.
(A-B) Real time qPCR analysis of axial progenitor markers in hESC- (SA001) (A) and hiPSC- (WTSli002) (B) -derived progenitors at Day 2, 3 and 4 of differentiation. Data are represented as mRNAs expression fold-changes to Day 0. **(C)** Immunostaining for axial progenitor markers on hiPSC (WTSli002)-derived Day 2, 3 and 4 progenitors. White square indicate the cells shown in higher magnification on the right of the panel Scale bars: 100µm (left), 40 µm right, magnification). **(D)** Hierarchical clustering showing transcriptional dynamic (z-score) of a subset of genes from Day 0 to Day 4 and regrouped through 4 different clusters. **(E-F)** Reactome pathway analysis of genes upregulated (fold change ⩾ 2.0, p-value < 0.05) between **(E)** Day 0 and Day 3 or **(F)** Day 0 and Day 4. **(G-I)** 20 most enriched genes in D2 and D3 progenitors versus hESC. Progenitors acquired a transcriptomic signature resembling murine axial progenitors. **(J)** Comparison of genes up-regulated between Day 0 and Day 3 (fold change ⩾ 2.0, p-value < 0.05) and “NMP-like genes” reported in (Frith et al., 2018). **(K)** Real time-PCR analysis of FGF signaling markers mRNAs in hiPSC (WTSli002) derived progenitors at Day 2, 3 and 4 of differentiation. Data are represented as mRNAs expression fold-changes to Day 0, shown as mean ± SD. Each circle is an independent biological replicate: n=5 (B, C), n=2 to 3 (K).

Figure S6

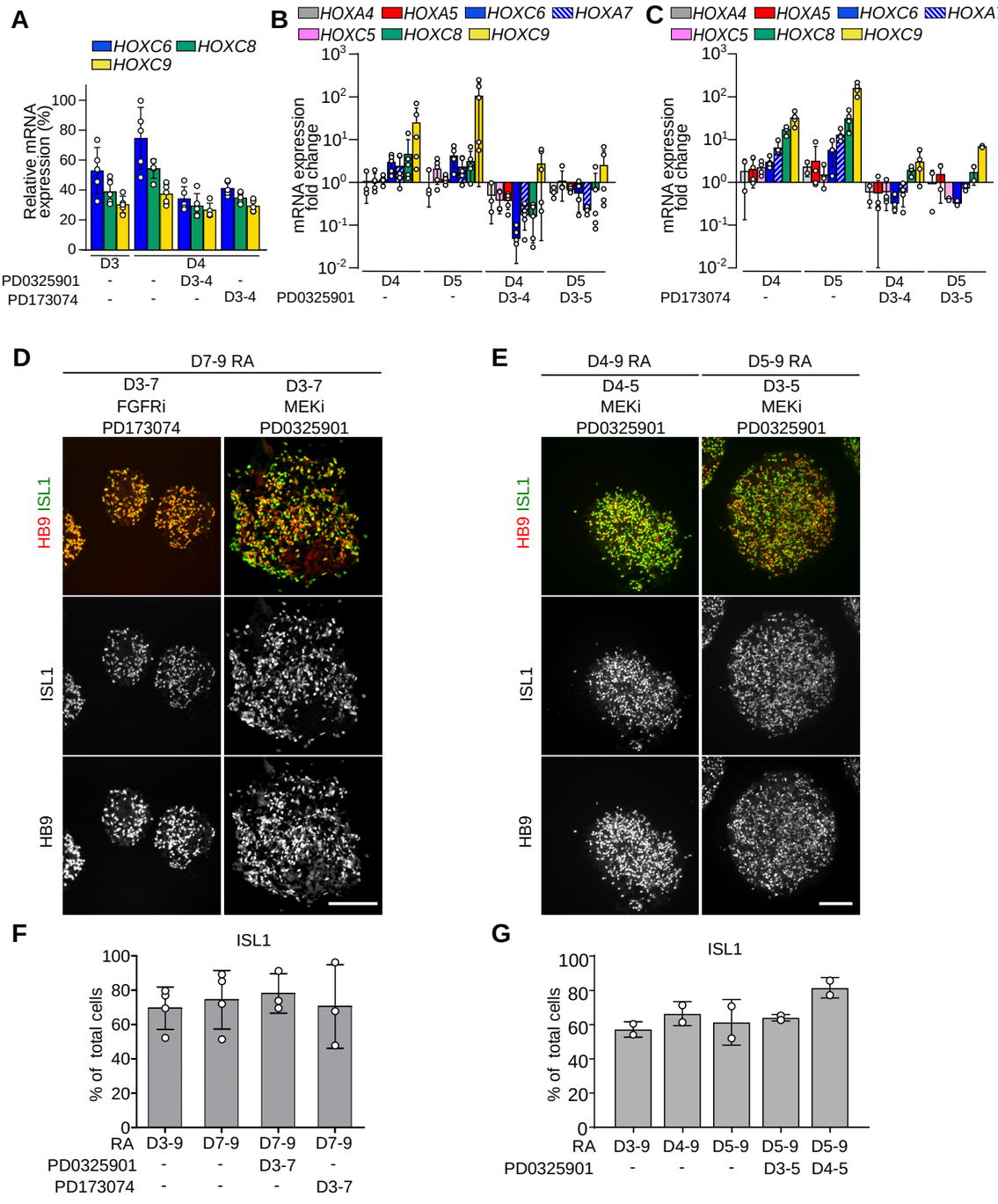

Figure S6 - FGFR and MEK1/2 inhibition in axial progenitors does not impact motor neuron specification

(A) Real time qPCR analysis of HOX mRNAs in hiPSC (WTSli002)-derived progenitors at Day 3, Day 4 and Day 5 of differentiation. Data are represented as relative expression to the highest expressed gene. MEK1/2 and FGFR inhibitors (PD173074), applied from Day 3 prevent the temporal increase in caudal HOX expression. **(B-C)** Real time PCR analysis of HOX mRNAs in progenitors at Day 4 and 5 of differentiation. Data are the same as in Fig.3B-C, but here represented as mRNA expression fold change to Day 3 controls to better visualize decreases in expression. MEK1/2 and FGFR inhibitors, applied from Day 3 prevent the temporal increase in caudal HOX expression and induce a repression of HOX genes compare to their initial expression level. **(D-E)** Immunostaining on Day 14 cryostat sections of embryoid bodies against ISL1 and HB9. Scale bars: 100µm. **(F-G)** Quantification of the proportion of ISL1 positive cells in Day 14 EBs from experiment presented respectively in A and B. Exposing axial progenitors to either FGFR or MEK1/2 inhibitors does not prevent the specification of motor neurons and have no effect on the proportion of ISL1+ and HB9+ cells. Data are shown as mean ± SD; Each circle is an independent biological replicate: n=5 (A), n=3 to 5 (B), n=4 (C), n=3 to 4 (E), n=2 (F).

Figure S7

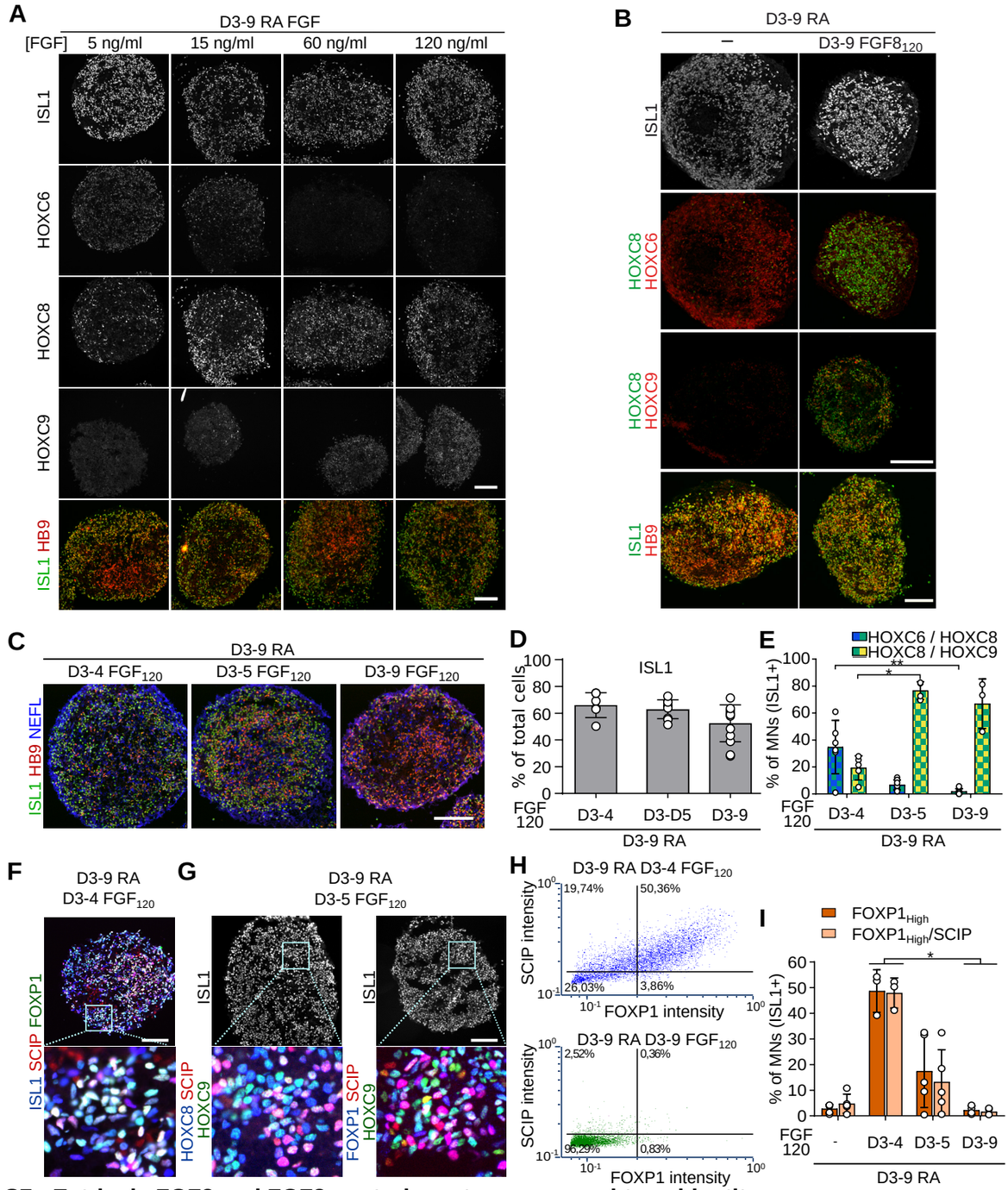

Figure S7 - Extrinsic FGF2 and FGF8 controls motor neuron subtype identity.

(A) Immunostaining on cryostat sections of hESC (SA001)-derived EBs at Day 14 of differentiation. Staining for ISL1, HOXC6, HOXC8 and HOXC9 to test the effect of varying FGF2 concentration on MN subtype identity. Scale bar: 100µm. **(B)** Immunostaining for ISL1, HB9, HOXC6, HOXC8, HOXC9 in control and upon addition of 120 ng/ml FGF8 between Day 3 and Day 9. Scale bar: 100µm. **(C-I)** Characterization on Day 14 of differentiation of the effect of varying FGF2 duration of exposure on MN generation and subtype identity. In all cases, FGF2 was added at Day 3 and the duration of exposure was modulated. **(C)** Immunostaining on cryostat sections of EBs for ISL1, HB9 and NEFL to test for MN specification. **(D)** Proportion of MNs on Day 14 of differentiation. **(E)** Quantification of HOXC6/HOX8/ISL1 and HOXC8/HOXC9/ISL1 co-expression. **(F-G)** Immunostaining for ISL1, SCIP and FOXP1 (F) or HOXC8/HOXC9/SCIP/ISL1 (G) aiming at characterizing the specification of MNs acquiring the identity of limb and digit innervating motor neurons. **(H)** Quantification of FOXP1high and FOXP1high/SCIP motor neurons using FCS software. Intensities of staining were extracted with Cell Profiler software and plotted using FCS Express software. FOXP1 weak and negative cells were defined on the FGF D3-9 condition. The gate was then reported on the other conditions. **(I)** Proportion of FOXP1high and FOXP1high/SCIP upon modulation of FGF2 treatment duration. All scale bars: 100µm. Data are shown as mean ± SD. Each circle is an independent biological replicate: n=3 to 9 (D), n=3 to 6 (E), n=3 to 5 (I). * if P ≤ 0.05 and ** if P ≤ 0.01. ANOVA with KW post hoc.

Figure S8

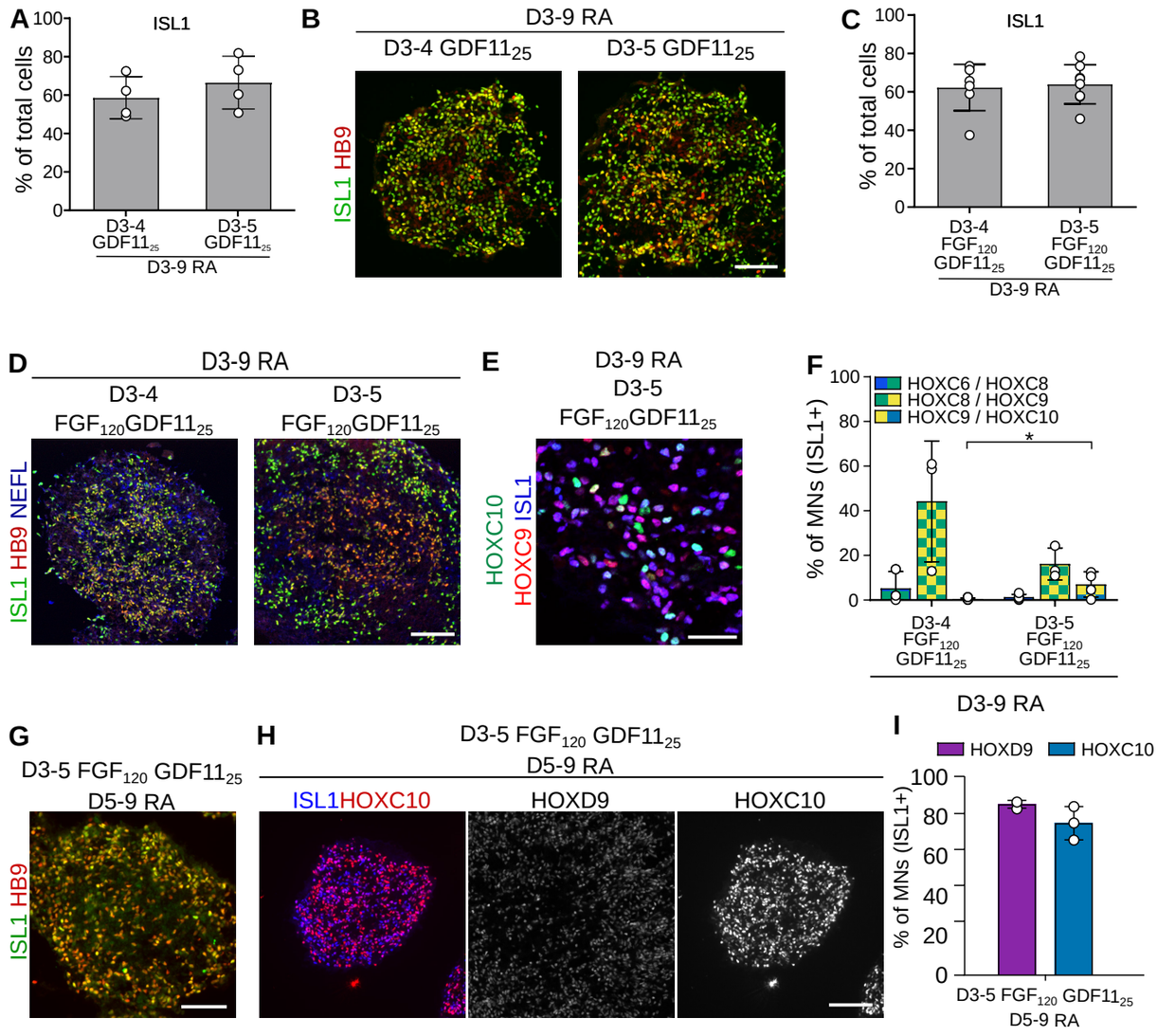

Figure S8 - FGF2 and GDF11 cooperate to induce caudal thoracic and lumbar motor neurons. RNA-seq analysis of in vitro derived axial progenitors. ***Related to Figure 2-4***

(A) Quantification of the percentage of MNs on Day 14 of differentiation upon addition of GDF11. GDF11 (25 ng/ml) was added on Day 3 for different durations. **(C)** Quantification of the percentage of MNs (ISL1+ cells) on Day 14 of differentiation upon addition of FGF2 and GDF11. FGF2 (120 ng/ml) and GDF11 (25 ng/ml) were added on Day 3 of differentiation for different durations. **(B,D)** Representative images of immunostainings for the motor neuron markers ISL1, HB9 (B) and the pan neuronal marker NEFL on cryostat sections of EBs on Day 14 of differentiation. Scale bars: 100µm. **(E)** Representative image of immunostaining for ISL1, HOXC9 and HOXC10 on cryostat sections of EBs on Day 14 of differentiation. Scale bar: 30µm. **(F)** Quantification of the percentage of HOXs co-expression in the indicated conditions. **(G-H)** Representative images of immunostainings for ISL1, HB9, HOXC9 and HOXC10 on cryostat sections of EBs on Day 14 of differentiation. Scale bars: 100µm. **(I)** Quantification of the percentage of HOXD9 and HOXC10 in the indicated conditions. Data are shown as mean ± SD. Each circle is an independent biological replicate: n=3 to 4 (A), n=4 (C), n=3 to 5 (F), n=3 (I). * if P ≤ 0.05. ANOVA with KW post hoc.

Table S1: normalized transcriptomic data

Click here to Download Table S1

Table S2: Differentially expressed genes between the different timepoints

Click here to Download Table S2

Table S3: Common genes enriched in axial progenitors in this study and in Frith et al.

Click here to Download Table S3

Table S4: Genes expressed in axial progenitors and in NMPs

Click here to Download Table S4

Table S5: small molecules, recombinant proteins, primers, antibodies

Click here to Download Table S5